The reversed chemical engine cycle with application to desalination processes

Bilal A. Qureshi [a], Syed M. Zubair [b,♣], Gregory P. Thiel [c], John H. Lienhard V [c]

[a]Center of Excellence for Scientific Research Collaboration with MIT, KFUPM Box # 1276

[b]Mechanical Engineering Department, KFUPM Box # 1474

King Fahd University of Petroleum & Minerals

Dhahran 31261, Saudi Arabia

[c]Rohsenow Kendall Heat Transfer Laboratory

Department of Mechanical Engineering,

Massachusetts Institute of Technology

Cambridge, MA 02139-4307, USA

ABSTRACT

In this paper, a novel thermodynamic cycle is proposed, termed the reversed chemical engine cycle. In the cycle, a net input of work is used to transfer mass from a low chemical potential reservoir to a high chemical potential reservoir. The cycle has two mass exchangers, a pump, and a turbine. The only irreversibility considered in the model is finite-rate mass transfer. Similar to the reversed Carnot cycle, expressions for the Performance Ratio (analogous to the Coefficient of Performance) are obtained under the condition of minimized power requirement for the endoreversible and, in turn, the reversible case. The reversed mass engine cycle is shown to be a special case of the reversed chemical engine. An equipartitioned hybrid forward osmosis reverse osmosis (FO–RO) system is considered as an example of the cycle.

♣ Corresponding author. Tel.: +966 13 860-3135. *E-mail address:* smzubair@kfupm.edu.sa.

Keywords: Reversed mass engine; Performance ratio; Reverse osmosis; Forward osmosis; Equipartition

1. Introduction

Reversible cycles provide an upper bound on performance parameters, e.g., thermal efficiency in Carnot heat engines and Coefficient of Performance (COP) in reverse Carnot cycles. In the latter, the cycle receives heat from the low-temperature reservoir and rejects heat to the high-temperature reservoir, which requires a net input of power. This power input is equal to the difference in the heat transfers, as required by the First Law of Thermodynamics. Two heat exchangers are used to transfer heat between the thermal reservoirs and the working fluid over an infinitesimal temperature difference. A typical example of such a cycle includes two other components in the cycle, a compressor and a turbine. In the reversible case, the overall cycle includes two isothermal and two isentropic processes [1,2].

When finite thermal resistances are included for the heat exchangers, efficiencies are reduced relative to the reversible case. In this so-called endoreversible case, the thermal efficiency and COP are determined under the conditions of maximum and minimum power, respectively, with the heat transfer process driven by a finite temperature difference. Real power plants or refrigeration/heat pump systems can have thermal efficiency and COP that are, respectively, greater or lesser than the endoreversible value [3–5].

Analogy is a powerful tool that can be used to solve problems and derive new ways of understanding. An important example is the use of electric circuit theory in solving heat transfer problems [6,7]. The maximum power relations for chemical engines have also been derived using analogies to heat engines. Applications range from chemical reactions and mass

exchangers to solid-state converters [8–11]. Even an analogy to thermal engine-driven heat pumps has been derived [12]. Design requirements for restrained chemical engines was provided by Miller *et al.* [13] using a fuel cell with a motor attachment as an example. Further information on current technologies for power generation using salinity gradients may be taken from Jia *et al.* [14] and Sharma *et al.* [15]. Recently, analogous to the Carnot heat engine, a reversible mass engine cycle was proposed by Sharqawy [16]. In this cycle, instead of heat exchangers, mass exchangers using semi-permeable membranes were used that allowed water to pass through but not other substances; other components included a pump and turbine. The same amount of mass was added to and rejected by the cycle. An expression for the reversible limit was established in which, instead of a temperature ratio, the process was characterized by pressure and concentration ratios. The cycle includes two isobaric and two constant concentration processes. An osmotic power plant using pressure-retarded osmosis, a type of salinity gradient engine, was envisaged as an application of the cycle.

The reverse Carnot cycle is the reversible cycle for refrigeration and heat pump systems (described above); and, therefore, by analogy the reversible mass engine cycle proposed by Sharqawy [16] can also be reversed. Thus, by extension, so can the isothermal chemical engine cycle. Generally speaking, such a cycle would receive some mass from a low-potential reservoir and reject the same mass to a high-potential reservoir, which would require a net power input (See Fig. 1). An example would be a desalination process, which transfers water from a saline mixture (low chemical potential) to a pure water reservoir (high chemical potential). The net power input would be equal to the difference in the energy transfers associated with the masses or the difference between the pump and turbine work. For the endoreversible chemical engine, two chemical exchangers of finite resistance would be used to transfer mass between the fixed

chemical potential reservoirs. In the case of a desalination process, the driving potential (the partial molar Gibbs energy of water) is represented in terms of differentials in the hydraulic and osmotic pressures [17,18]. The other two components of the cycle are a pump and a turbine.

It should be noted that to reduce the energy consumption of desalination systems, hybrids of known desalination processes are being considered that work in a cycle [19]. Therefore, there is a need to evaluate the efficiency of these hybrids on a thermodynamic basis. Reversible and endoreversible forms of these hybrid cycles can help to achieve this by establishing limiting values, which is not yet addressed in the literature.

The objective of the current work is to introduce the concept of the reversed chemical engine cycle and its components. The cycle will be driven by chemical potential differences and analyzed in analogy with classical heat engines. Additionally, we aim to derive the relevant thermodynamic relations and performance metrics, the most important of which are the reversible limit of performance and the limit under the condition of the minimum power requirement for the endoreversible (internally reversible) case.

2. Reverse chemical engine: Endoreversible and reversible case

An isothermal (endoreversible) reverse chemical engine is shown in Figs. 1 and 2. Taking the resistance to mass transfer (such as a membrane in a mass exchanger) on the high-potential mass transfer branch as the control volume, we may write the mass transfer, N_H, as

$$N_H = h_H(\mu_H - \mu_H)t_H \tag{1a}$$

The above equation assumes that the mass transfer and chemical potential difference are linearly proportional to each other [9]. In Eq. (1a), μ_H represents the high-side chemical potential of the

transferred species in the reservoir, μ_H' is the chemical potential of that species in the engine fluid on the high-potential mass transfer branch, t_H is the residence time of the fluid in the chemical exchanger, and h_H is the proportionality constant and can be called the conductance for mass flow. Multiplying both sides of Eq. (1a) by μ_H', we get [20]

$$G_H = \mu_H' N_H = \mu_H' h_H (\mu_H' - \mu_H) t_H \tag{1b}$$

where G_H represents the Gibbs free energy of the transferred species on the high-potential mass transfer branch. Equation (1a) and/or Eq. (1b) may be considered an analogy with respect to the heat transfer to the hot reservoir in an endoreversible heat pump or refrigerator. Similarly, for the low-potential mass transfer branch, we may write

$$N_L = h_L(\mu_L - \mu_L')t_L \tag{2a}$$

$$G_L = \mu_L' N_L = \mu_L' h_L (\mu_L - \mu_L') t_L \tag{2b}$$

This is analogous to the heat transfer from the cold reservoir in an endoreversible heat pump or refrigerator. Now, conservation of mass results in:

$$N_H = N_L = N \tag{3a}$$

By combining Eqs. (1b), (2b), and (3a), we may write [20]

$$\frac{G_H}{\mu_H'} = \frac{G_L}{\mu_L'} \tag{3b}$$

Equation (3b) is an analogy to the Clausius inequality for an endoreversible heat pump/refrigerator. Now, taking the reverse chemical engine as the control volume, the internally reversible work input (W) for the chemical engine is given by [9]

$$W = N(\mu'_H - \mu'_L) \tag{4a}$$

so that we may say

$$W = G_H - G_L \tag{4b}$$

The above equation is analogous to the first law of thermodynamics applied to an endoreversible heat pump/refrigerator. Further, this equation represents the usual understanding of least work of separation for an isothermal and isobaric system [21,22].

Let us consider that the objective of the cycle is to produce pure component. Since the chemical exchanger on the high-side produces it, therefore, by analogy to the COP of a heat pump, we may define a Performance Ratio as the metric for our engine:

$$PR_{CE,H} = \frac{G_H}{W} = \frac{G_H}{G_H - G_L} \tag{5}$$

Substituting Eq. (1b) and (2b) into Eq. (3b), we get

$$\frac{t_H}{t_L} = \frac{h_L}{h_H}\frac{(m_L - m_L^{\phi})}{(m_H^{\phi} - m_H)} \tag{6}$$

The power input to the engine can be expressed as

$$\dot{W} = \frac{G_H - G_L}{t_H + t_L} \tag{7}$$

Substituting Eq. (1b) and (2b) in Eq. (7) and then using Eq. (6) to eliminate the time ratio (t_H / t_L), we get

$$\dot{W} = \frac{h_L h_H xy(\mu_H - \mu_L + x + y)}{(h_H x + h_L y)} \tag{8}$$

where $x = (\mu_H' - \mu_H)$ and $y = (\mu_L - \mu_L')$.

Now we seek to minimize the power requirement under the constraint of mass conservation given in Eq. (3a). Taking the derivative of Eq. (8) with respect to *x* and equating it to zero gives us

$$-h_L y(\mu_H - \mu_L' + x + y) = x(h_H x + h_L y) \tag{9a}$$

Taking the derivative with respect to *y* and equating it to zero gives us:

$$-h_H x(\mu_H - \mu_L + x + y) = y(h_H x + h_L y) \tag{9b}$$

Dividing Eq. (9a) by Eq. (9b), we find after simplifying

$$\frac{y}{x} = \sqrt{\frac{h_H}{h_L}} \tag{10}$$

Substituting Eq. (10) into Eq. (6), we get

$$\frac{t_H}{t_L} = \sqrt{\frac{h_L}{h_H}} \tag{11}$$

Eq. (11) is analogous to the time ratio found in the reverse Carnot cycle for the endoreversible case [23]. We also find that, by combining Eqs. (6) and (11), the value of the chemical potential of the fluid on the low side under the condition of minimum power is given by:

$$\mu_L' = \mu_L - \sqrt{\frac{h_H}{h_L}}(\mu_H' - \mu_H) \tag{12}$$

The performance ratio (Eq. (5)), based on Eq. (3a-b) can be written as:

$$PR_{CE,H} = \left[1 - \frac{G_L}{G_H}\right]^{-1} = \left[1 - \frac{\mu_L}{\mu_H}\right]^{-1} \tag{13}$$

Substituting Eq. (12) into Eq. (13), we get

$$PR^{*}_{CE,H} = \left[1 - \frac{\mu_L - \sqrt{h_H/h_L}\,(\mu'_H - \mu_H)}{\mu'_H}\right]^{-1} = \left[1 - \frac{\mu_L - \sqrt{h_H/h_L}\,\Delta\mu_H}{\Delta\mu_H + \mu_H}\right]^{-1} \tag{14}$$

It can be seen that this maximum performance ratio depends upon the reservoir chemical potentials, μ_H and μ_L, the chemical potential difference of the high-side fluid $\Delta\mu_H$, and the ratio of the proportionality constants, i.e. h_H and h_L. In the reversible case, the driving force becomes infinitesimal, i.e. $\mu'_H \to \mu_H$ and $\mu'_L \to \mu_L$. Therefore, the limit of PR, in Eq. (13), as μ'_H and μ'_L approach μ_H and μ_L, respectively, is:

$$PR_{CE,H,\text{rev}} = \left[1 - \frac{\mu_L}{\mu_H}\right]^{-1} \tag{15}$$

Now, if we consider a process wherein the chemical exchange process on the low-side is of interest to us, then the Performance Ratio may be written by analogy to the COP of a refrigerator as follows:

$$PR_{CE,L} = \frac{G_L}{W} = \frac{G_L}{G_H - G_L} \tag{16a}$$

Using Eq. (3a-b), this may be rearranged to give

$$PR_{CE,L} = \left[\frac{G_H}{G_L} - 1\right]^{-1} = \left[\frac{\mu_H}{\mu_L} - 1\right]^{-1} \tag{16b}$$

The chemical potential of the fluid on the high side is determined by calculations similar to previous case:

$$\mu'_H = \mu_H + \sqrt{\frac{h_L}{h_H}}(\mu_L - \mu'_L) \tag{17}$$

Substituting Eq. (17) into Eq. (16b), we get

$$PR^*_{CE,L} = \left[\frac{\mu_H + \sqrt{h_L/h_H}(\mu_L - \mu'_L)}{\mu'_L} - 1\right]^{-1} = \left[\frac{\mu_H + \sqrt{h_L/h_H}\Delta\mu_L}{\mu_L - \Delta\mu_L} - 1\right]^{-1} \tag{18}$$

It can be seen that the performance ratio depends upon the reservoir chemical potentials, μ_H and μ_L, the chemical potential difference on the low-side fluid $\Delta\mu_L$, and the ratio of the proportionality constants, i.e. h_H and h_L. Similar to the previous case, the limit of PR, in Eq. (16b), as μ'_H and μ'_L approach μ_H and μ_L, respectively, is:

$$PR_{CE,L,rev} = \left[\frac{\mu_H}{\mu_L} - 1\right]^{-1} \tag{19}$$

Finally, due to the clear analogy with the reverse Carnot cycle, the following result can easily be shown:

$$PR_{CE,L} + 1 = PR_{CE,H} \tag{20}$$

For an isothermal system, the *total* entropy generation for the reverse chemical engine can be written as [24]:

$$S_{gen} = \frac{(\mu_H - \mu_L)N - W}{T} \tag{21a}$$

so that the irreversibility, *I*, is given by:

$$I = TS_{gen} = \left(\mu_H - \mu_L\right) N - W \tag{21b}$$

2.1 Reverse mass engine: A special case

An isothermal (endoreversible) reverse mass engine is shown in Figs. 3 and 4. Taking the control volume around the resistance to mass transfer (such as a semi-permeable membrane) on the high-potential mass transfer branch (See Fig. 3), we may write the mass transfer as:

$$m_H = K_H \left(\Delta P - \Delta\pi\right) t_H \tag{22a}$$

This may be re-arranged as follows:

$$m_H = K_H \left(\left(P - \pi\right)'_H - \left(P - \pi\right)_H\right) t_H \tag{22b}$$

Multiplying and dividing by the density of the high-side reservoir, ρ_H , we get

$$m_H = \left(r_H K_H\right)\left(\frac{\left(P - \rho\right)'_H}{r_H} - \frac{\left(P - \rho\right)_H}{r_H}\right) t_H = \left(r_H K_H\right)\left(\frac{\Delta P_H}{r_H} - \frac{\Delta \rho_H}{r_H}\right) t_H \tag{23a}$$

The above equation assumes that mass transfer and hydro-osmotic potential, i.e. $\left(P - \rho\right)/r$, differences are linearly proportional to each other. In Eq. (23a), $\left(P - \rho\right)_H / r_H$ represents the high-side hydro-osmotic potential reservoir, $\left(P - \rho\right)^{¢}_H / r_H$ is the hydro-osmotic potential of the engine fluid on the high-potential mass transfer branch, t_H is the residence time of the fluid in the mass exchanger, and K is the proportionality constant called the permeability coefficient. The equation is also re-arranged so that it shows the difference between the hydrostatic and osmotic

pressure differences, since this is the common way it is mentioned in literature [25–27]. In keeping with the analogy, the hydro-osmotic potential will be used. Now, multiplying both sides of Eq. (23a) by $\left(P - \rho\right)_H^{\text{¢}} \Big/ r_H$, we get

$$\tilde{W}_H = \frac{\left(P-\pi\right)_H^{'}}{\rho_H} m_H = \frac{\left(P-\pi\right)_H^{'}}{\rho_H}\left(\rho_H K_H\right)\left(\frac{\left(P-\pi\right)_H^{'}}{\rho_H} - \frac{\left(P-\pi\right)_H}{\rho_H}\right) t_H \tag{23b}$$

where $\tilde{W}_H$, a hydro-osmotic work term, is defined as shown. This can be determined by taking the enthalpy difference of the end states (See Appendix A). Equation (23a) and/or Eq. (23b) may be considered an analogy with respect to heat transfer to the hot reservoir in an endoreversible heat pump or refrigerator. More importantly, let us consider the following substitutions in Eqs. (23(a)-(b)):

$$\frac{\left(P-\pi\right)}{\rho} = \mu, \rho K = h, m = N, \tilde{W} = G \tag{24}$$

It becomes clear that the mass exchanger just described is simply a special case of the chemical exchanger in a chemical engine discussed in the previous section. Similarly, for the low-potential mass transfer branch, we may write

$$m_L = \left(\rho_L K_L\right)\left(\frac{\left(P-\pi\right)_L}{\rho_L} - \frac{\left(P-\pi\right)_L^{'}}{\rho_L}\right) t_L \tag{25a}$$

$$\tilde{W}_L = \frac{\left(P-\pi\right)_L^{'}}{\rho_L} m_L = \frac{\left(P-\pi\right)_L^{'}}{\rho_L}\left(\rho_L K_L\right)\left(\frac{\left(P-\pi\right)_L}{\rho_L} - \frac{\left(P-\pi\right)_L^{'}}{\rho_L}\right) t_L \tag{25b}$$

This is an analogy with respect to the heat transfer from the cold reservoir in an endoreversible heat pump or refrigerator. Clearly, the substitutions mentioned in Eq. (24) would have a similar result as for the low-side mass transfer branch. Now, conservation of mass results in:

$$m_H = m_L = m \tag{26a}$$

We may then write using Eqs. (23b) and (25b)

$$\frac{\tilde{W}_H}{\left(\left(P-\pi\right)'/\rho\right)_H} = \frac{\tilde{W}_L}{\left(\left(P-\pi\right)'/\rho\right)_L} \tag{26b}$$

If we take ρ_w as the density of pure water and assume that salt water density varies linearly with salt (solute) concentration (w), we can write

$$r_H = r_w\left(1+w_H\right) \tag{27a}$$

$$r_L = r_w\left(1+w_L\right) \tag{27b}$$

It should be noted that *w* is the mass of solutes per total mass of solution in kg/kg.

$$\frac{\tilde{W}_H}{\left(\left(P-\pi\right)'/\left(1+w\right)\right)_H} = \frac{\tilde{W}_L}{\left(\left(P-\pi\right)'/\left(1+w\right)\right)_L} \tag{28}$$

Equation (28) is an analogy to the Clausius inequality for a reversible process applied to an endoreversible heat pump/refrigerator. Now, taking the reverse mass engine as the control volume, the (net) work input (W_{net}) for the mass engine is given by

$$W_{net} = \tilde{W}_H - \tilde{W}_L \tag{29}$$

The above equation is analogous to the first law of thermodynamics applied to an endoreversible heat pump/refrigerator.

Now, let us assume that the mass exchanger on the high-side is of interest to us. Therefore, if we consider the Performance Ratio as a performance metric for our engine, we may write the following equation analogous to the COP of a heat pump:

$$PR_{ME,H} = \frac{\tilde{W}_H}{W_{net}} = \frac{\tilde{W}_H}{\tilde{W}_H - \tilde{W}_L} \tag{30}$$

Equation (30) also represents a special case of Eq. (5). Similar to the chemical engine, we seek to minimize the power requirement for the constraint of mass conservation given in Eq. (26a). Choosing the appropriate substitutions from Eq. (24), the time ratio from Eq. (11) is:

$$\frac{t_H}{t_L} = \sqrt{\frac{(rK)_L}{(rK)_H}} \tag{31}$$

while the hydro-osmotic potential of the fluid on the low side is given by:

$$\frac{(P-\pi)'_L}{\rho_L} = \frac{(P-\pi)_L}{\rho_L} - \sqrt{\frac{(\rho K)_H}{(\rho K)_L}}\left(\frac{(P-\pi)'_H}{\rho_H} - \frac{(P-\pi)_H}{\rho_H}\right) \tag{32}$$

The performance ratio [Eq. (30)] can be written as:

$$PR_{ME,H} = \left[1 - \frac{\tilde{W}_L}{\tilde{W}_H}\right]^{-1} = \left[1 - \frac{\left((P-\pi)'/\rho\right)_L}{\left((P-\pi)'/\rho\right)_H}\right]^{-1} \tag{33}$$

Substituting Eq. (32) into Eq. (33), we obtain the performance ratio at the condition of minimum power:

$$PR^{*}_{ME,H} = \left[1 - \frac{\frac{(P-\pi)_L}{\rho_L} - \sqrt{\frac{(\rho K)_H}{(\rho K)_L}} \left(\frac{(P-\pi)'_H}{\rho_H} - \frac{(P-\pi)_H}{\rho_H} \right)}{\frac{(P-\pi)'_H}{\rho_H}} \right]^{-1} \tag{34a}$$

which can be simplified to

$$PR^{*}_{ME,H} = \left[1 - \frac{\rho_H}{\rho_L} \frac{(P-\pi)_L - \sqrt{(\rho_L K_H)/(\rho_H K_L)} \left((P-\pi)'_H - (P-\pi)_H \right)}{(P-\pi)'_H} \right]^{-1} \tag{34b}$$

As in the reversed chemical engine cycle, the limit of PR, in Eq. (33), as $\left((P-\pi)' / \rho \right)_H$ and $\left((P-\pi)' / \rho \right)_L$ approach $\left((P-\pi)/\rho \right)_H$ and $\left((P-\pi)/\rho \right)_L$, respectively, is:

$$PR_{ME,H,rev} = \left[1 - \frac{\left((P-\pi)/\rho \right)_L}{\left((P-\pi)/\rho \right)_H} \right]^{-1} \tag{35}$$

This can also be derived by substitution of Eq. (24) into Eq. (15).

Now, if we consider a process wherein the mass exchange process on the low-side is of interest to us, then the Performance Ratio may be written analogous to the COP of a refrigerator as follows:

$$PR_{ME,L} = \frac{\tilde{W}_L}{W_{net}} = \frac{\tilde{W}_L}{\tilde{W}_H - \tilde{W}_L} \tag{36a}$$

Similar to Eq. (33), we may write in this case

$$PR_{ME,L} = \left[\frac{\tilde{W}_H}{\tilde{W}_L} - 1\right]^{-1} = \left[\frac{\left(\left(P-\pi\right)/\rho\right)'_H}{\left(\left(P-\pi\right)/\rho\right)'_L} - 1\right]^{-1} \tag{36b}$$

The hydro-osmotic potential of the fluid on the high side is determined similar to previous case:

$$\frac{\left(P-\pi\right)'_H}{\rho_H} = \frac{\left(P-\pi\right)_H}{\rho_H} + \sqrt{\frac{\left(\rho K\right)_L}{\left(\rho K\right)_H}}\left(\frac{\left(P-\pi\right)_L}{\rho_L} - \frac{\left(P-\pi\right)'_L}{\rho_L}\right) \tag{37}$$

Substituting Eq. (37) into Eq. (36b), we get

$$PR^{*}_{ME,L} = \left[\frac{\dfrac{\left(P-\pi\right)_H}{\rho_H} + \sqrt{\dfrac{\left(\rho K\right)_L}{\left(\rho K\right)_H}}\left(\dfrac{\left(P-\pi\right)_L}{\rho_L} - \dfrac{\left(P-\pi\right)'_L}{\rho_L}\right)}{\dfrac{\left(P-\pi\right)'_L}{\rho_L}} - 1\right]^{-1} \tag{38}$$

which can easily be manipulated into a form similar to Eq. (34b). As in the previous case, the limit of PR, in Eq. (36b), as $\left(\left(P-\pi\right)'/\rho\right)_H$ and $\left(\left(P-\pi\right)'/\rho\right)_L$ approach $\left(\left(P-\pi\right)/\rho\right)_H$ and $\left(\left(P-\pi\right)/\rho\right)_L$, respectively, is:

$$PR_{ME,L,rev} = \left[\frac{\left(\left(P-\pi\right)/\rho\right)_H}{\left(\left(P-\pi\right)/\rho\right)_L} - 1\right]^{-1} \tag{39}$$

Finally, similar to Eq. (20), due to the clear analogy with the reverse Carnot cycle, the following result can easily be shown:

$$PR_{ME,L} + 1 = PR_{ME,H} \tag{40}$$

3. Results and Discussion

In Fig. 4, the hydro-osmotic potential lines are horizontal (as in an equipartitioned process [28,29]) and this is the analog of the reversed Carnot cycle. In thermodynamics textbooks such as [1,2], gas refrigeration cycles, also called the reversed Brayton cycle (See Fig. 5), are introduced as internally reversible cycles in which the temperature lines are not horizontal. Furthermore, an open-cycle form of it meant as an application for aircraft cooling systems is also discussed (See Fig. 6). Following this line of thought, the reversed mass engine discussed previously would have hydro-osmotic potential lines that are not horizontal (See Fig. 7). The fact that these lines are not horizontal represents the typical situation in desalination systems. The lines are not horizontal because the outgoing mass transfer increases the salinity of the working fluid in the RO mass exchanger [30] on the high-side and, thus, continuously decreases the difference between the (constant) hydraulic and osmotic pressures. The opposite occurs in the PRO mass exchanger on the low side where the incoming mass of liquid (equal to the outgoing mass) decreases the salinity of the working fluid and, thus, continuously increases the difference between the hydraulic and osmotic pressures. If the FO/PRO mass exchanger in Fig. 7 is removed, it would result in an open-cycle application of the reversed mass engine.

The cycle indicates that it is possible to set up hybrid desalination systems and measure their performance. An example of this would be the RO-FO hybrid. An experimental setup was found in the recent work of Zaviska *et al.* [31] incorporating this. In this application, forward osmosis (low-side mass exchanger) was used as a pre-treatment for reverse osmosis (high-side

mass exchanger) for a brackish water feed that had high scaling potential (See Fig. (1a) of [31]). Another example found in the literature was an FO exchanger in which RO works as a regeneration system in order to concentrate the diluted draw [19]. An energetic analysis of this hybrid was performed by McGovern and Lienhard V [32]. It is interesting to note that Wijmans and Baker [33] mentioned that diverse processes such as dialysis, gas permeation, pervaporation and reverse osmosis can be described by a single unified approach using the solution-diffusion model. Based upon this, it is plausible to assume that the proposed cycle can incorporate these applications as well. Also, since regeneration is used in systems such as gas refrigeration cycles [1,2] as well as heat pump applications [34,35], the analogous concept applied to the cyclic process shown in the work of Zaviska *et al.* [31] may prove useful. But this will be the focus of future work. Also, a comparison of Figs. 4 and 7 indicates that if the mass exchange processes in Fig. 7 are equipartitioned [28], it would result in Fig. 4. Therefore, the performance of an equipartitioned RO-FO or RO-PRO hybrid (See Fig. 8) desalination system can be evaluated from the mathematical framework provided in this work. Further thoughts are mentioned in Appendix B.

It is important to note that, in the (reversed) Carnot heat exchanger cycle, the vertical axis is occupied by the absolute temperature and, thus, it cannot be negative. This is not necessarily true for the hydro-osmotic potential in the mass engine cycle. As an example, the well-known work of Loeb [36] shows a PRO module in which the hydro-osmotic pressure difference $(P - p)$ is negative for the draw side while it is nearly zero for the feed side.

For the purpose of showing applicability of the proposed model, examples for the chemical and mass engine cycles are presented below:

3.1 Illustrative example: Chemical engine cycle

For the purpose of demonstration, we will assume that the product of the chemical exchanger on the high-side is of interest to us. Therefore, Eq. (14) will be used to determine the endoreversible performance ratio while Eq. (15) will be used for its reversible value. We arbitrarily choose the chemical potential of the high-side reservoir $\mu_H = 100$ J/mol while the chemical potential difference on the high-side $\Delta\mu_H = 20$ J/mol and the ratio of the proportionality constants, h_H / h_L, is taken as unity. The chemical potential of the low-side reservoir, μ_L, is varied, from 5 to 65 J/mol, to help illustrate the behavior of both performance ratios with respect to each other.

Substituting the above-mentioned values into Eqs. (14) and (15), Fig. 9 shows, in general terms, the behavior of the reversed chemical engine model where the high-side chemical potential exchanger is of interest. As can be seen, the reversible PR is greater than the endoreversible PR. The difference between them increases as the chemical potential for the low-potential reservoir increases. The behavior is very similar to the case of the endoreversible heat pump [23]. A similar example can be constructed if the low-side chemical exchanger is of interest to us, in which case, Eqs. (18) and (19) will be used.

3.2 Illustrative example: Mass engine cycle

Let us consider an equipartitioned RO-PRO hybrid (See Fig. 8) at the minimum power requirement condition. For the purpose of demonstration, we will assume that the product (i.e. pure water) of the mass exchanger on the high-side (i.e. the RO module) is of interest to us.

Therefore, Eq. (34a) can be used to determine the endoreversible performance ratio while Eq. (35) will be used for its reversible value. The system temperature is assumed to be 25 °C. The high-potential reservoir is taken as pure water at atmospheric pressure i.e. $(P_H - \pi_H) = 101.3\,\text{kPa}$ and $\rho_H = 996.9\,kg/m^3$. The low-potential reservoir is assumed to be brackish water with a salinity of 10 g/kg so that $\rho_L = 1005\,kg/m^3$ while the difference between the hydraulic and osmotic pressures $(P_L - \pi_L)$ is taken as 7 kPa [36]. Substituting these values into Eq. (35), we find the value of PR for the reversible case to be 1.074. Now, the conditions for an equipartitioned seawater feed RO desalination system at 50% recovery ratio are given by Thiel *et al.* [29]. Table 3 of [29] shows that $(P-\pi)'_H = 2160\,\text{kPa}$. The ratio of the proportionality constants (h_H/h_L) may be taken as 1.5 [31]. Based upon this, the model in Section 2.1 allows for determining the conditions for the draw solution of the PRO module by substitution into Eq. (32) such that we find $\left(P-\pi\right)'_L \Big/ \rho_L = -2.522$. Substituting relevant values into Eq. (34a), we calculate the value of PR for the endoreversible case to be 0.462. Finally, Fig. 10 is the result of varying the difference between the hydraulic and osmotic pressures of the low-potential reservoir $(P_L - \pi_L)$ from 5 to 50 kPa. This demonstrates that the general behavior is similar to that predicted by the chemical engine cycle in Fig. 9.

4. Conclusions

A new thermodynamic cycle is proposed, termed the reversed chemical engine cycle. It uses a net input of work to transfer mass from a low chemical potential reservoir to a high chemical

potential reservoir. The cycle consists of two mass exchangers, a pump and a turbine. In general, the reversible limit and the endoreversible expressions (at the condition of minimum power requirement) for the performance ratios are found to be analogous to the reversed Carnot cycle for a refrigerator and heat pump. For the reversed chemical engine, the performance ratio depends upon the reservoir chemical potentials, chemical potential difference of the fluid on the side of interest and the ratio of the proportionality constants. For the reversed mass engine, processes such as RO as well as hybrids with processes such as FO and PRO are applications of this cycle. Some specific conclusions are as follows:

- A new term called the hydro-osmotic work is derived that can be determined by taking the enthalpy difference of the end states during which this work transfer occurs.
- For the reversed mass engine, an analogy to the Clausius inequality for a reversible process applied to an endoreversible heat pump/refrigerator was found:

$$\frac{\tilde{W}_H}{\left(\left(P-\pi\right)'/\left(1+w\right)\right)_H} = \frac{\tilde{W}_L}{\left(\left(P-\pi\right)'/\left(1+w\right)\right)_L}$$

- Analogous to the reversed Carnot cycle, the reversible PR was demonstrated to be greater than the endoreversible PR.
- Further work is needed to extend the concept to varying chemical potential.

Nomenclature

G Gibbs free energy of transferred species (J)

h conductance for mass flow (mol^2/J s)

I irreversibility (J)

K permeability coefficient (kg/s kPa)

m mass flux of transferred species (kg)

N mole flux of transferred species (mol)

P hydraulic pressure (kPa)

PR performance ratio

Q heat transfer (J)

S salinity (g/kg)

S_{gen} total entropy generation (J/ K)

s specific entropy (J/kg K)

T temperature (K)

t residence time (s)

W internally reversible work (J)

$\tilde{W}$ hydro-osmotic work (J)

$\dot{W}$ power input (W)

w solute concentration (kg/kg)

Greek symbols

Δ difference

μ chemical potential of transferred species (J/mol)

π osmotic pressure (kPa)

ρ density (kg/m^3)

Superscripts

$()^*$ at condition of minimum power for endoreversible case

$()'$ value of property in the engine fluid

Subscripts

CE chemical engine

H high side

i i^{th} component

L low side

ME mass engine

net net

rev reversible case

w pure water

Abbreviations

COP coefficient of performance

FO forward osmosis

PRO pressure retarded osmosis

RO reverse osmosis

Acknowledgements

The authors acknowledge support from the King Fahd University of Petroleum and Minerals (KFUPM) through the Center for Clean Water and Clean Energy at MIT and KFUPM under Project Number R15-CW-11. Syed Zubair also acknowledges support from KFUPM through the project IN151001.

Appendix A. Determination of hydro-osmotic work ($\tilde{W}$)

The change in Gibbs free energy for a mixture can be written as [37]:

$$dG = -SdT + VdP + \sum_{i=1}^{k} \mu_i dN_i \tag{A1}$$

Then, for an isothermal process,

$$dG = \sum_{i=1}^{k} \mu_i dN_i + VdP \tag{A2}$$

We know that H = U + PV and, therefore, if we take the derivative, we can write

$$dH = dU + PdV + VdP \tag{A3}$$

The first Gibbs relation when extended to include chemical potential gives us [37]

$$dU = TdS - PdV + \sum_{i=1}^{k} \mu_i dN_i \tag{A4}$$

Substituting Eqs. (A3) and (A2) into Eq. (A4), we get

$$dH = TdS + dG \tag{A5}$$

If the process is isentropic,

$$dH = dG \tag{A6}$$

Simply substituting from Eq. (24), we get

$$dH = d\tilde{W} \tag{A7}$$

This shows that the hydro-osmotic work term encountered in section 3 can be determined by taking the enthalpy difference between the two states during which it occurs.

Another way to come to a similar conclusion is by simply considering the fact that, by applying an energy balance on the engine, the net work of the mass engine cycle is given by:

$$W_{net} = W_p - W_t = \tilde{W}_H - \tilde{W}_L \tag{A8}$$

It is also clear that the pump and turbine work terms can be determined by enthalpy differences. Therefore, a simple re-arrangement of these enthalpy terms would show that the hydro-osmotic work terms are determined by enthalpy differences of the two states during which these transfers occur.

Appendix B. Mass engine cycle with an energy recovery device

The use of pressure exchangers as an energy recovery device in desalination systems is well known. These devices perform better than hydro-turbines owing to their higher efficiencies [38]. This suggests that, in the mass engine cycle proposed here (Figs. 4 and 8), the turbine could be replaced with a pressure exchanger (See Fig. B.1). Most of the diluted draw flow is extracted to match the brine flow from the RO module. The rest of the flow, equal to that added in the FO module, is directed to the first pump. Most of the diluted flow after state 4 would receive a boost in pressure from the brine at state 2. After this, the flow would go through the second pump and then mix with the discharge of the first one to complete the process. This would reduce the electricity consumption (and net work input) of the system and, hence, a higher PR would be achieved.

References

[1] Y.A. Cengel, M.A. Boles, Thermodynamics: An Engineering Approach, 7th ed., McGraw-Hill Inc., 2010.

[2] R.E. Sonntag, E. Borgnakke, G.J. Van Wylen, Fundamentals of Thermodynamics, 5th ed., Wiley, New York, 1998.

[3] J. Chen, Z. Yan, G. Lin, B. Andresen, On the Curzon-Ahlborn efficiency and its connection with the efficiencies of real heat engines, Energy Convers. Manag. 42 (2001) 173–181.

[4] A. Bejan, Advanced Engineering Thermodynamics, 3rd ed., John Wiley & Sons, Inc., New Jersey, 2006.

[5] A. de Vos, Endoreversible thermodynamics of solar energy conversion, Oxford University Press, Oxford, UK, 1992.

[6] J.H. Lienhard IV, J.H. Lienhard V, A Heat Transfer Textbook, 4th ed., Dover Publications, Mineola, NY, 2011. http://ahtt.mit.edu.

[7] L.C. Thomas, Heat Transfer-Professional Version, 2nd ed., Capstone Publishing Corporation, 1999.

[8] J.M. Gordon, Maximum work from isothermal chemical engines, J. Appl. Phys. 73 (1993) 8. doi:10.1063/1.353835.

[9] L. Chen, F. Sun, C. Wu, J. Yu, Performance characteristics of isothermal chemical engines, Energy Convers. Manag. 38 (1997) 1841–1846.

[10] J.M. Gordon, V.N. Orlov, Performance characteristics of endoreversible chemical engines, J. Appl. Phys. 74 (1993) 5303–5309. doi:10.1063/1.354253.

[11] N. Boon, R. van Roij, “Blue energy” from ion adsorption and electrode charging in sea and river water, Mol. Phys. 109 (2011) 1229–1241. doi:10.1080/00268976.2011.554334.

[12] G. Lin, J. Chen, B. Hua, Optimal analysis on the performance of a chemical engine-driven chemical pump, Appl. Energy. 72 (2002) 359–370.

[13] S.L. Miller, M.N. Svrcek, K.-Y. Teh, C.F. Edwards, Requirements for designing chemical engines with reversible reactions, Energy. 36 (2011) 99–110. doi:10.1016/j.energy.2010.11.002.

[14] Z. Jia, B. Wang, S. Song, Y. Fan, Blue energy: Current technologies for sustainable power generation from water salinity gradient, Renew. Sustain. Energy Rev. 31 (2014) 91–100. doi:10.1016/j.rser.2013.11.049.

[15] K. Sharma, Y. Kim, S. Yiacoumi, J. Gabitto, H.Z. Bilheux, L.J. Santodonato, et al., Analysis and simulation of a blue energy cycle, Renew. Energy. 91 (2016) 249–260. doi:10.1016/j.renene.2016.01.044.

[16] M.H. Sharqawy, Mass engine cycle, in: Proc. ASME 2014 Int. Mech. Eng. Congr. Expo., Montreal, Quebec, Canada, 2014: pp. 1–6.

[17] D.R. Paul, Reformulation of the solution-diffusion theory of reverse osmosis, J. Memb. Sci. 241 (2004) 371–386. doi:10.1016/j.memsci.2004.05.026.

[18] M. Wilf, L. Awerbuch, The guidebook to membrane desalination technology: Reverse osmosis, nanofiltration and hybrid systems : Process, design, applications and economics, Balaban Desalination Publications, L'Aquila, Italy, 2007.

[19] E.W. Tow, R.K. McGovern, J.H. Lienhard V, Raising forward osmosis brine concentration efficiency through flow rate optimization, Desalination. 366 (2015) 71–79. doi:10.1016/j.desal.2014.10.034.

[20] S. Sieniutycz, J. Jezowski, Energy Optimization in Process Systems, Elsevier, Oxford, UK, 2009.

[21] K. Mistry, J. Lienhard, Generalized Least Energy of Separation for Desalination and Other Chemical Separation Processes, Entropy. 15 (2013) 2046–2080. doi:10.3390/e15062046.

[22] P.W. Atkins, L. Jones, Chemical principles: The quest for insight, 4th editio, Palgrave Macmillan, Basingstoke, 2007.

[23] C.H. Blanchard, Coefficient of performance for finite speed heat pump, J. Appl. Phys. 51 (1980) 2471–2472.

[24] G. Lin, J. Chen, E. Brück, Irreversible chemical-engines and their optimal performance analysis, Appl. Energy. 78 (2004) 123–136. doi:10.1016/j.apenergy.2003.07.001.

[25] R.W. Baker, Membrane Technology and Applications, 2nd ed., John Wiley & Sons, Ltd, Chichester, UK, 2004. doi:10.1002/9781118359686.

[26] J. Kucera, Reverse Osmosis, John Wiley & Sons, 2010.

[27] H.T. El-Dessouky, H.M. Ettouney, Fundamentals of Salt Water Desalination, Elsevier B.V., Amsterdam, 2002.

[28] D. Tondeur, E. Kvaalent, Equipartition of entropy production. An optimality criterion for transfer and separation processes, Ind. Eng. Chem. Res. 26 (1987) 50–56.

[29] G.P. Thiel, R.K. McGovern, S.M. Zubair, J.H. Lienhard V, Thermodynamic equipartition for increased second law efficiency, Appl. Energy. 118 (2014) 292–299. doi:10.1016/j.apenergy.2013.12.033.

[30] L.D. Banchik, M.H. Sharqawy, J.H. Lienhard, Effectiveness-mass transfer units (ε-MTU) model of a reverse osmosis membrane mass exchanger, J. Memb. Sci. 458 (2014) 189–198. doi:10.1016/j.memsci.2014.01.039.

[31] F. Zaviska, Y. Chun, M. Heran, L. Zou, Using FO as pre-treatment of RO for High scaling potential brackish water: Energy and performance optimisation, J. Memb. Sci. 492 (2015) 430–438. doi:10.1016/j.memsci.2015.06.004.

[32] R.K. McGovern, J.H. Lienhard V, On the potential of forward osmosis to energetically outperform reverse osmosis desalination, J. Memb. Sci. 469 (2014) 245–250. doi:10.1016/j.memsci.2014.05.061.

[33] J.G. Wijmans, R.W. Baker, The solution-diffusion model: a review, J. Memb. Sci. 107 (1995) 1–21. doi:10.1016/0376-7388(95)00102-I.

[34] A.J. White, Thermodynamic analysis of the reverse Joule–Brayton cycle heat pump for domestic heating, Appl. Energy. 86 (2009) 2443–2450. doi:10.1016/j.apenergy.2009.02.012.

[35] H. Yuan, C.-L. Zhang, Regenerated air cycle potentials in heat pump applications, Int. J. Refrig. 51 (2015) 1–11. doi:10.1016/j.ijrefrig.2014.11.016.

[36] S. Loeb, Large-scale power production by pressure-retarded osmosis, using river water and sea water passing through spiral modules, Desalination. 143 (2002) 115–122. doi:10.1016/S0011-9164(02)00233-3.

[37] S.I. Sandler, Chemical and engineering thermodynamics, Third ed., John Wiley & Sons, Inc., 1999.

[38] H. Ettouney, M. Wilf, Commercial Desalination Technologies, in: A. Cipollina, G. Micale, L. Rizzuti (Eds.), Seawater Desalin. Conv. Renew. Energy Process., Springer-Verlag Berlin Heidelberg, 2009. doi:10.1007/978-3-642-01150-4.

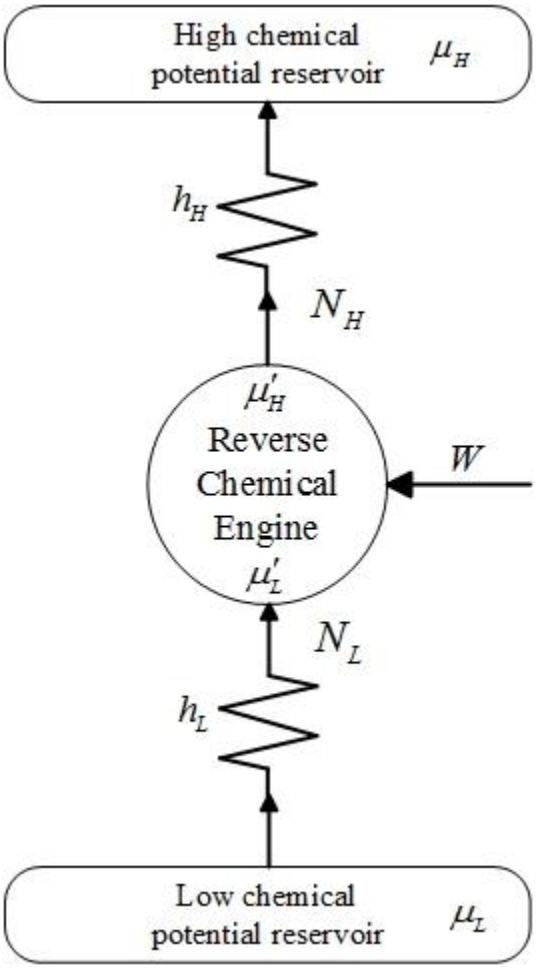

Fig. 1. Endoreversible reverse chemical engine

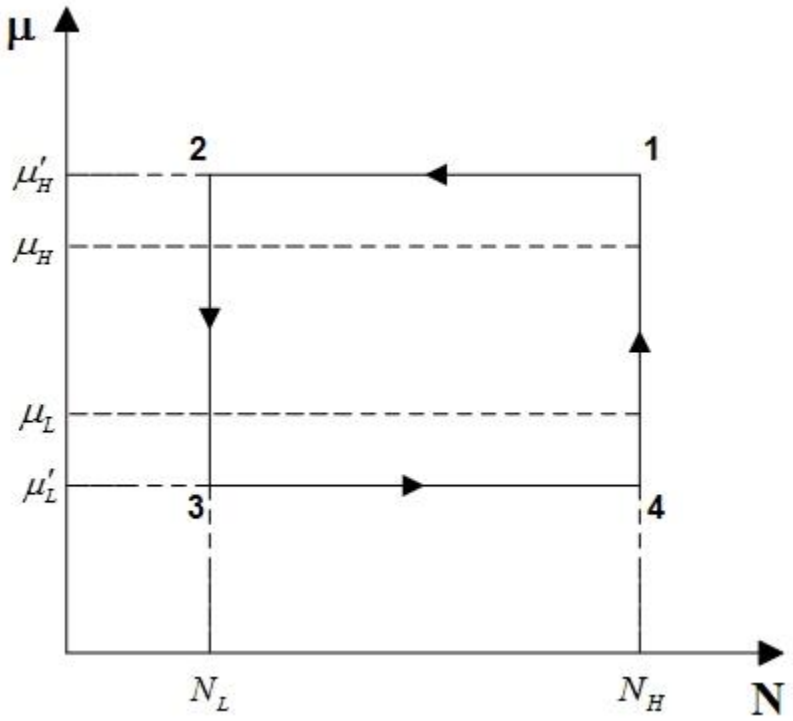

Fig. 2. Chemical potential-mole flux diagram of a (endoreversible) reverse chemical engine

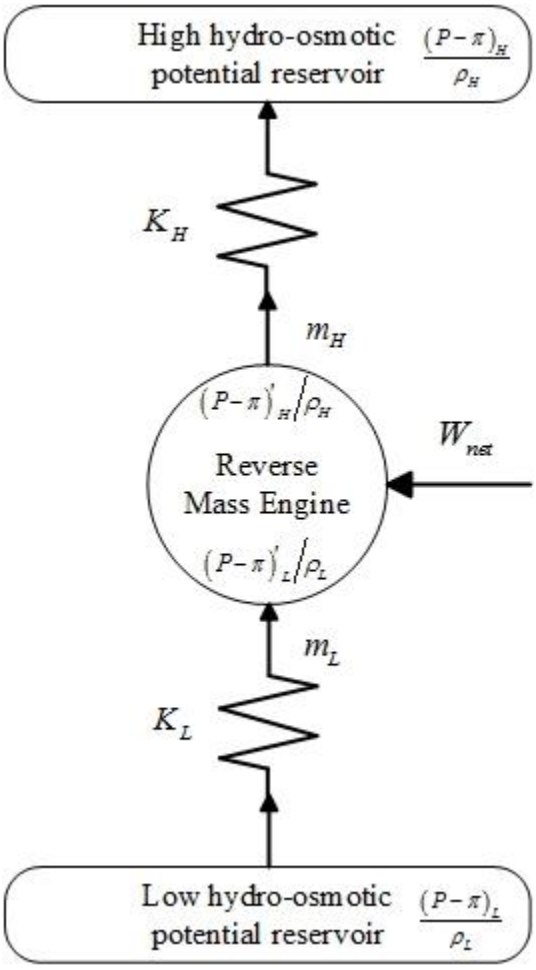

Fig. 3. Endoreversible reverse mass engine

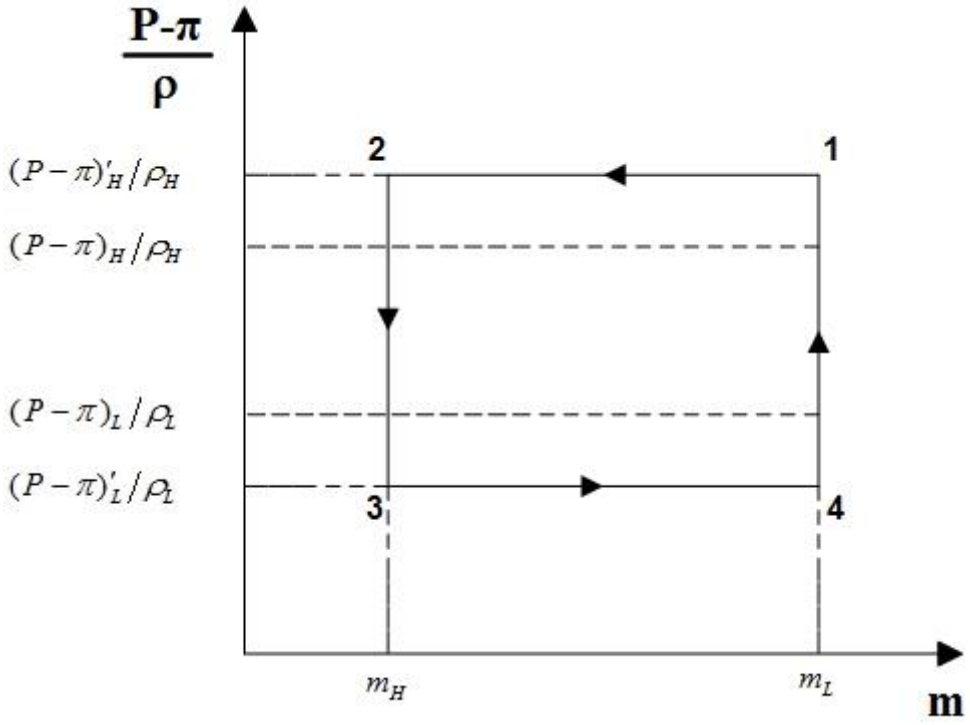

Fig. 4. Hydro-osmotic potential-mass transfer diagram of a (endoreversible) reverse mass engine

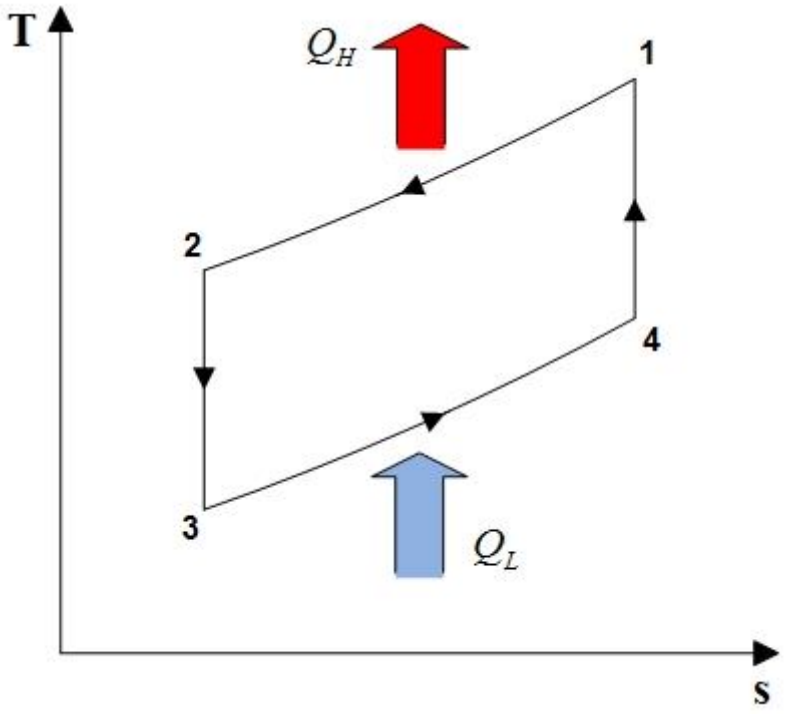

Fig. 5. Temperature-entropy diagram of a simple reversed Brayton cycle

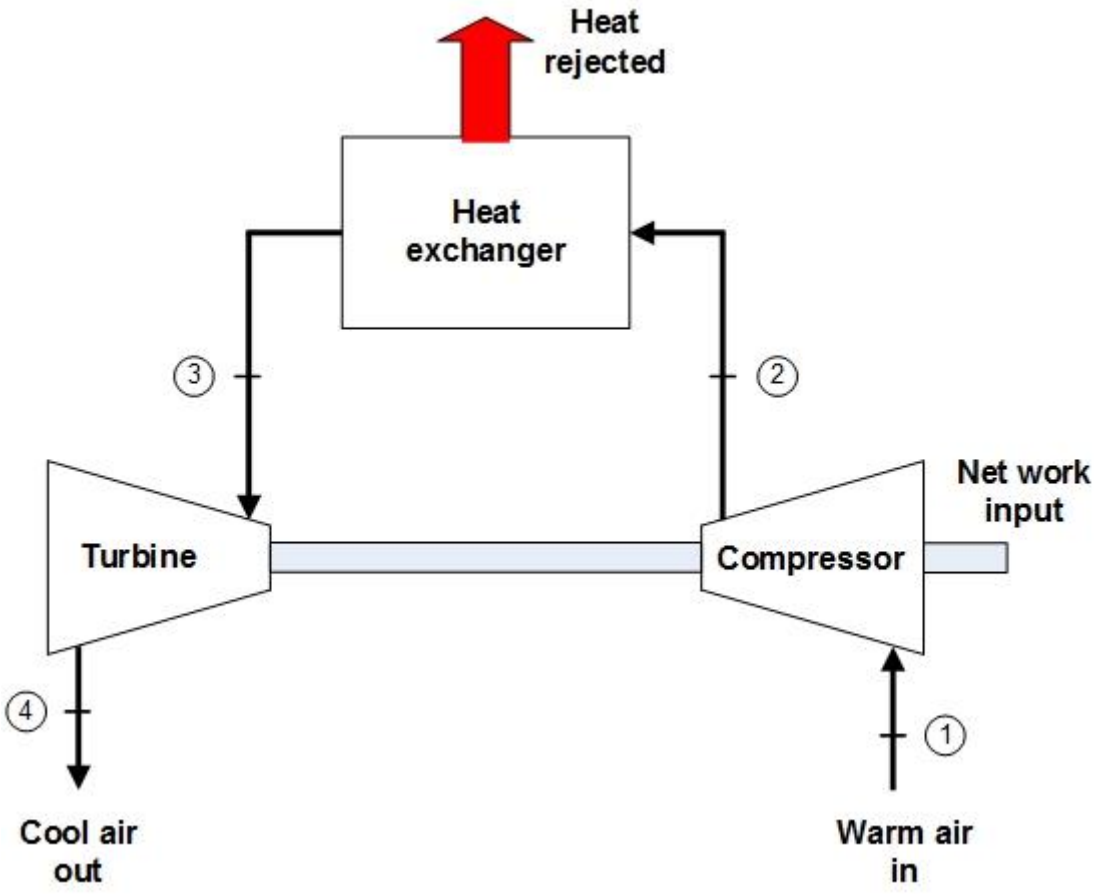

Fig. 6. Open-cycle cooling system

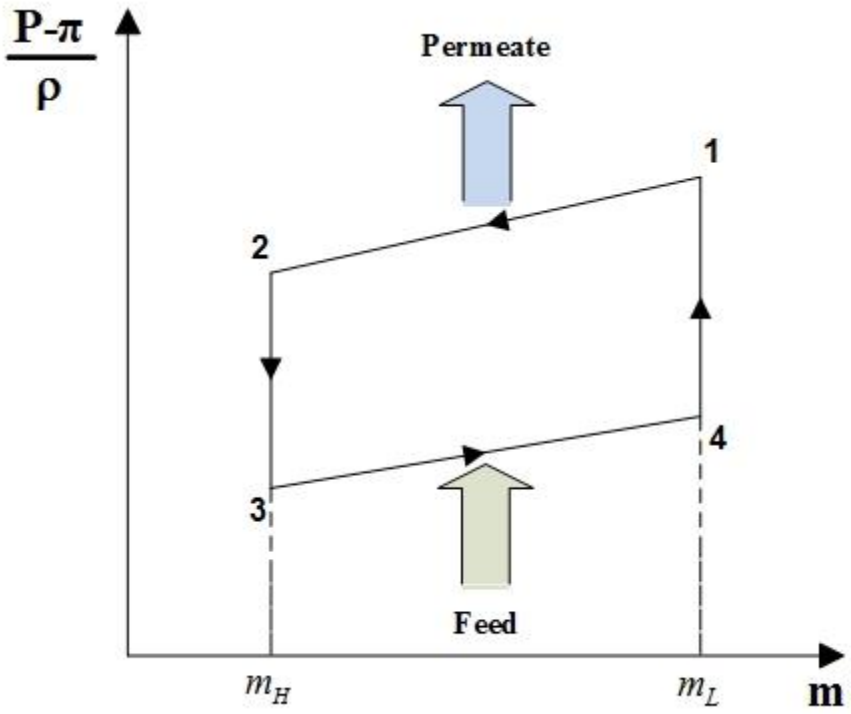

Fig. 7. Hydro-osmotic potential-mass transfer diagram of an actual RO-FO/PRO based reversed mass engine cycle

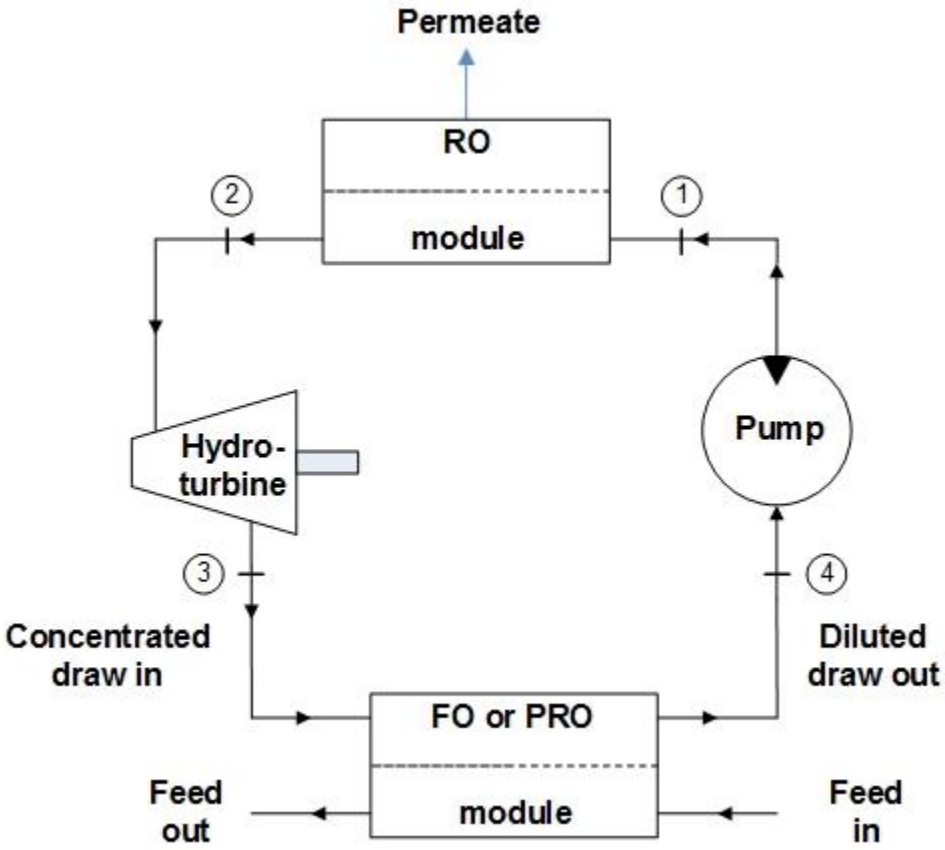

Fig. 8. RO-FO/PRO hybrid desalination system

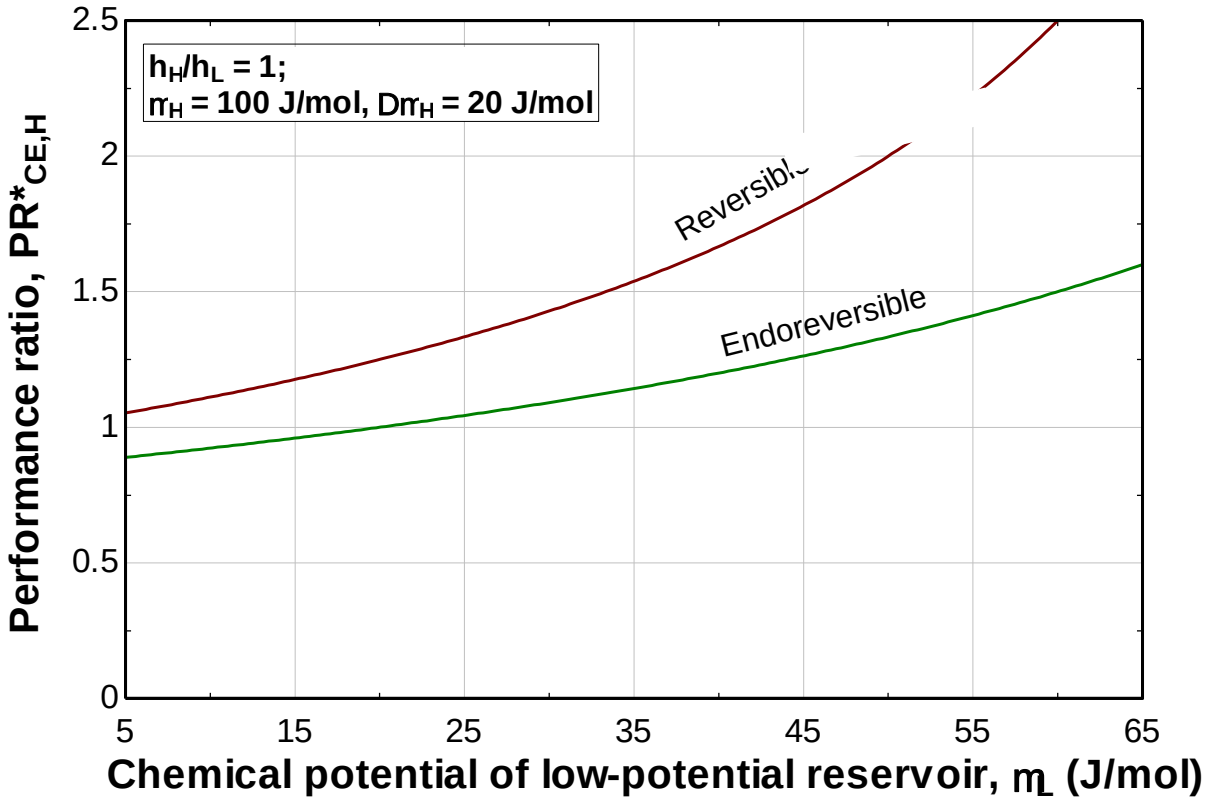

Fig. 9. Comparison of reversible and endoreversible performance ratio for a chemical engine cycle

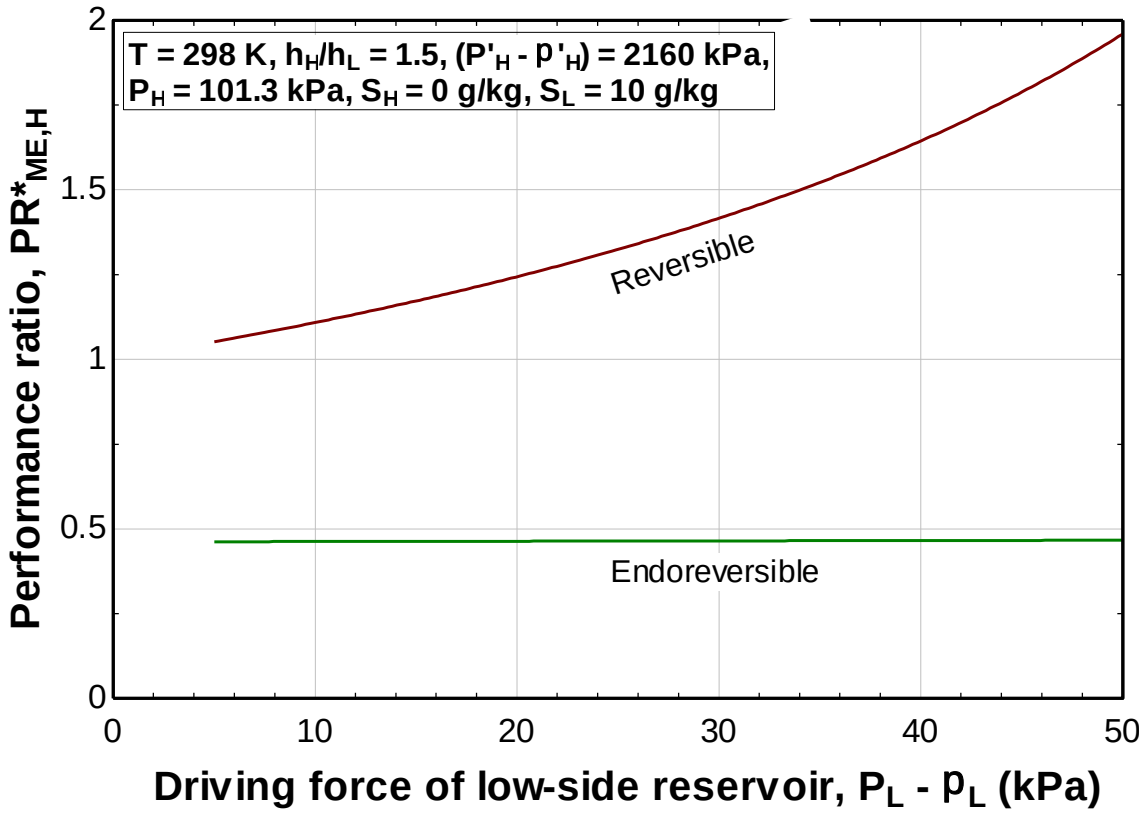

Fig. 10. Comparison of reversible and endoreversible performance ratio for a mass engine cycle

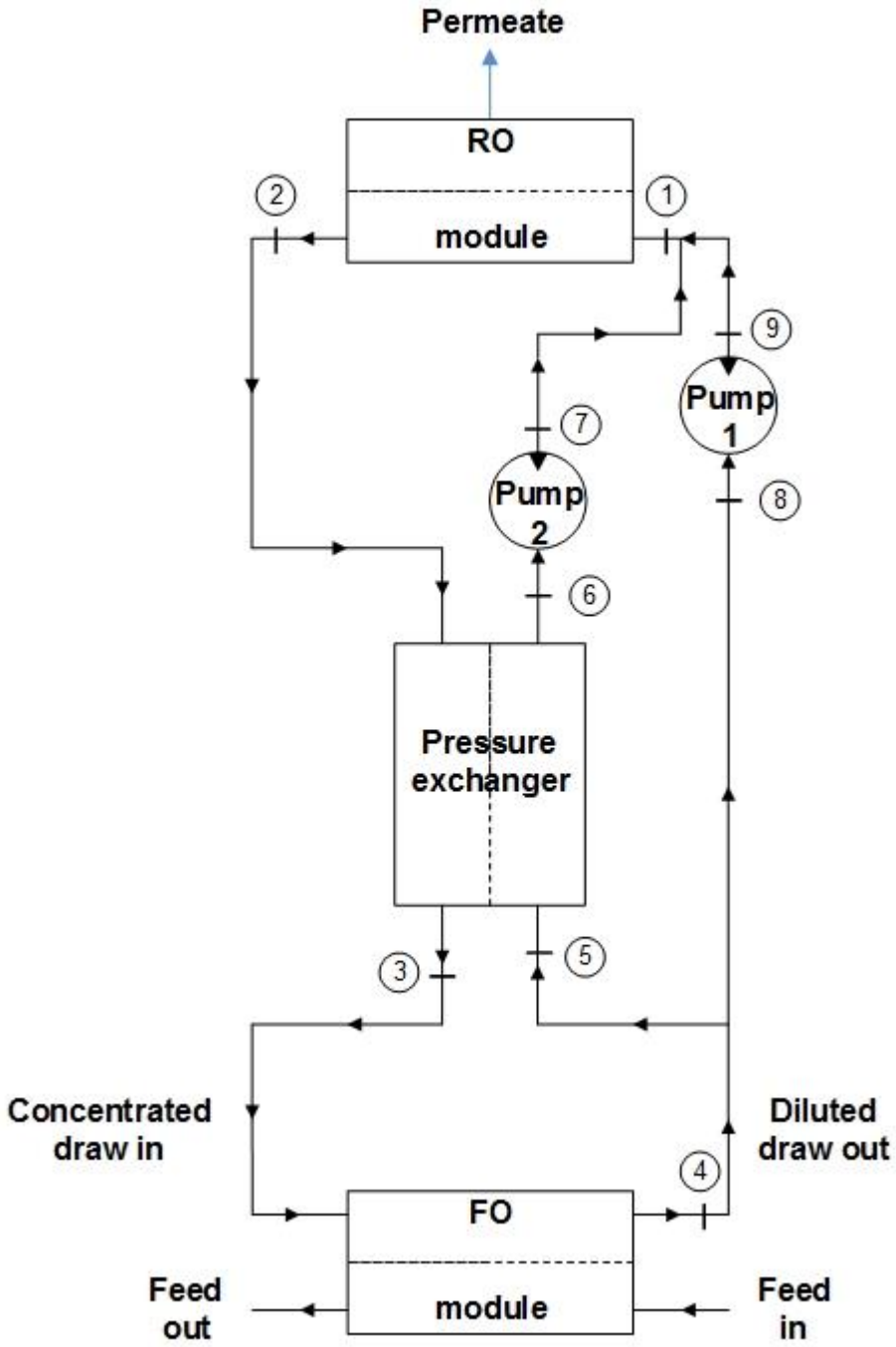

Fig. B.1. RO-FO based reversed mass engine cycle with pressure exchanger

Figure Captions

Fig. 1. Endoreversible reverse chemical engine

Fig. 2. Chemical potential-mole flux diagram of a (endoreversible) reverse chemical engine

Fig. 3. Endoreversible reverse mass engine

Fig. 4. Hydro-osmotic potential-mass transfer diagram of a (endoreversible) reverse mass engine

Fig. 5. Temperature-entropy diagram of a simple reversed Brayton cycle

Fig. 6. Open-cycle aircraft cooling system

Fig. 7. Hydro-osmotic potential-mass transfer diagram of an actual RO-FO/PRO based reversed mass engine cycle

Fig. 8. RO-FO/PRO hybrid desalination system

Fig. 9. Comparison of reversible and endoreversible performance ratio for a chemical engine cycle

Fig. 10. Comparison of reversible and endoreversible performance ratio for a mass engine cycle

Fig. B.1. RO-FO based reversed mass engine cycle with pressure exchanger